Journal of Alloys and Compounds 513 (2012) 277–281

Contents lists available at SciVerse ScienceDirect

Journal of Alloys and Compounds

journal homepage: www.elsevier.com/locate/jallcom

Enhanced flux pinning in MOD-YBCO films with co-doping of $BaZrO_3$ and Y_2O_3 nanoparticles

Fazhu Ding[a,*], Hongwei Gu[a], Teng Zhang[a], Hongyan Wang[a], Fei Qu[a], Shaotao Dai[a], Xingyu Peng[a], Jiangli Cao[b]

[a] Key Laboratory of Applied Superconductivity, Institute of Electrical Engineering, Chinese Academy of Sciences, Beijing 100190, China
[b] Institute for Advanced Materials and Technology, University of Science and Technology Beijing, Beijing 100083, China

ARTICLE INFO

Article history:
Received 7 September 2011
Received in revised form 8 October 2011
Accepted 13 October 2011
Available online 21 October 2011

PACS:
74.76.Bz
81.15.Lm

Keywords:
YBCO films
BZO/Y_2O_3 doping
Flux pinning
TFA-MOD

ABSTRACT

A combined $BaZrO_3$ (BZO) and Y_2O_3 nanoparticles has been achieved in $YBa_2Cu_3O_{7-x}$ (YBCO) films by metalorganic deposition using trifluoroacetates (TFA-MOD). The formation of integrated nanoparticles increases the critical current density (J_c) of Y_2O_3/BZO doped-YBCO films while keeping the critical transition temperature (T_c) close to that in the pure YBCO films. The YBCO film with 7.0 mol.% BZO and 7.0 mol.% Y_2O_3 showed T_c value of 90 K and J_c value of 6.5 mA/cm^2 at self-field (0 T, 77 K). The strongly enhanced flux pinning over a wide range of magnetic field can be attributed to the combined different crystal structures of BZO and Y_2O_3 created by optimized TFA-MOD conditions.

1. Introduction

Remarkable progress has been obtained in the fabrication technology of the second generation (2G) high temperature superconducting (HTS) wire in recent years. More than 1000 m-long $YBa_2Cu_3O_{7-x}$ (YBCO) tapes with critical current (I_c) values higher than 250 A/cm-width were realized. Improvement in their performance that can translate to lower cost for a given application has recently become topics of the most intense research on HTS coated conductors.

In 1990s, the most pedestrian factors that limit the critical current density (J_c) in YBCO coated conductor are material imperfections and the weak-link effect. Once these problems have been solved, the property that determines the ability of coated conductors to carry supercurrent is referred to as 'flux pinning'. As the coherence length in YBCO superconductors is very small ($\xi_{ab} \approx 2$ nm, $\xi_c \approx 0.5$ nm), only nanosized microstructure within the YBCO matrix can act as effective pinning centers [1]. Approaches to obtaining significant improvements in J_c have been realized for YBCO films, including decoration of substrate surfaces by nanoparticles [2–5], the addition of oxide nanoparticles [6–9], multilayering of YBCO with second-phase materials [10–12], mixed rare-earth elements doping [13–15], and an intentional deviation from the 123 stoichiometry [16,17]. Among these strategies for the enhancement J_c of YBCO films, introduction of nanoparticles in YBCO films is the most promising approach for its valuable advantages such as high efficiency and easy control. MacManus-Driscoll et al. [18] attempted first to improve J_c of YBCO films by introduction of $BaZrO_3$ (BZO) nanoparticles in films grown by pulsed laser deposition (PLD). Gutiérrez et al. [19] demonstrated that BZO particles in YBCO films grown by metalorganic deposition using trifluoroacetates (TFA-MOD) process exhibited a gigantic effectiveness for magnetic flux pinning. In this case, BZO nanodots were randomly dispersed in the YBCO matrix and an overall increase in J_c occurred. Subsequently, significant efforts have been made to introduce other perovskites compounds such as $BaHfO_3$ [20], $BaSnO_3$ [21,22], and $BaIrO_3$ [23] in YBCO films. And lately the integration of different compounds to improving flux pinning of YBCO film was reported [24,25]. In the present study, we fabricated YBCO films consisting of BZO and Y_2O_3 nanostructures by TFA-MOD process. The correlation between the microstructural features and the superconducting properties is discussed.

* Corresponding author. Tel.: +86 10 82547146; fax: +86 10 82547137.
E-mail address: dingfazhu@mail.iee.ac.cn (F. Ding).

0925-8388/$ – see front matter © 2011 Elsevier B.V. All rights reserved.
doi:10.1016/j.jallcom.2011.10.035

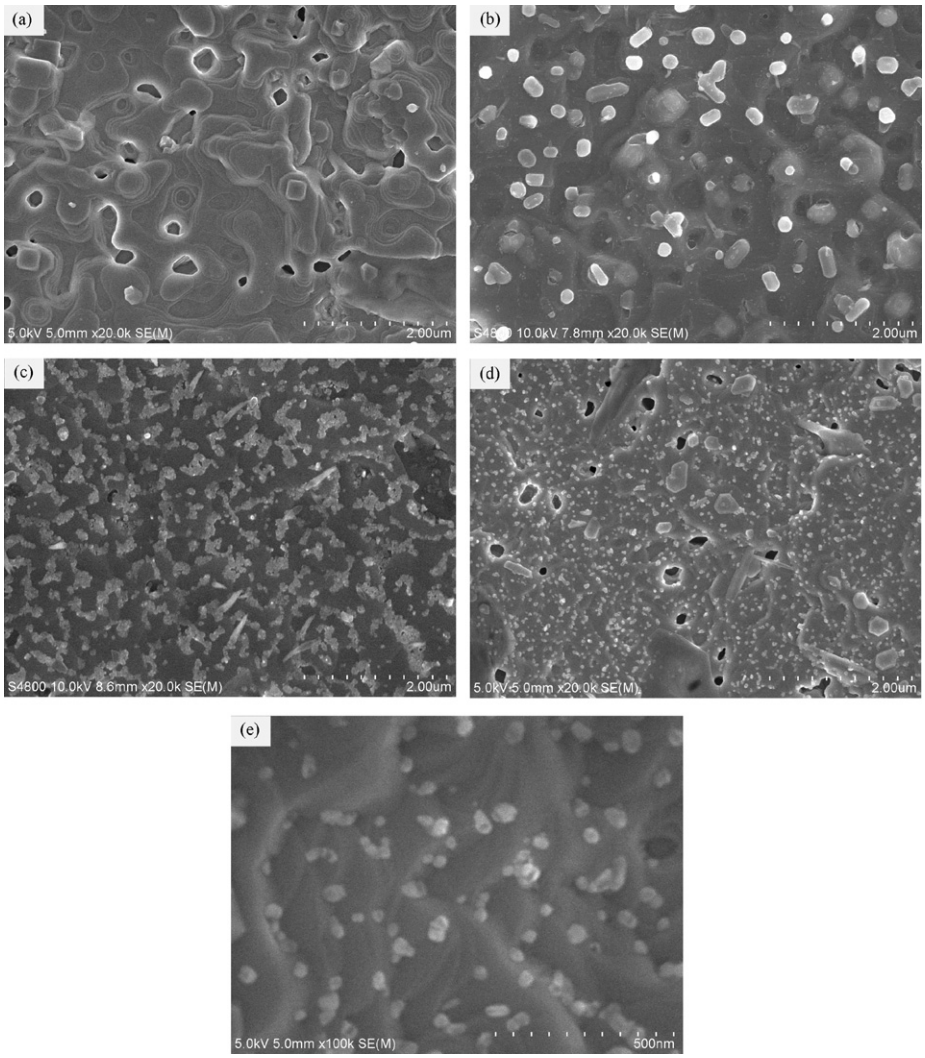

Fig. 1. SEM micrographs of YBCO films prepared with different solutions: (a) conventional TFA precursor solution, (b) 7 mol.% excess acetates of yttrium TFA precursor solution, (c) 7 mol.% Zr acetylacetonate TFA precursor solution, and (d and e) 7 mol.% excess acetates of yttrium and 7 mol.% Zr acetylacetonate TFA precursor solution.

2. Experimental details

The precursor solution for YBCO film with BZO and Y_2O_3 was prepared by dissolving the acetates of yttrium, barium and copper and Zr acetylacetonate with stoichiometric proportions in de-ionized water with an excess stoichiometric quantity of trifluoroacetic acid at room temperature. The concentrations of Y_2O_3 and BZO in the investigated YBCO films were adjusted by controlling the acetates of yttrium and the Zr acetylacetonate in the precursor solution, respectively. The resulting aqueous solution was refluxed for 10 h and then dried to a semisolid state, and then re-dissolved in methanol for drying. Finally, the residue was dissolved in sufficient methanol to get the final trifluoroacetate precursor solution with a concentration of 1.5 mol/L. The solution was coated onto 10 mm × 5 mm (0 0 *h*)-oriented LAO substrates at a spinning rate of 3000 rpm for 2 min. Then the samples were put in a quartz tube within a horizontal furnace. Coated films were calcined at the temperature up to 400 °C in 4.2% humidified oxygen with a flow rate of 500 cc/min. The calcined films were fired at 820 °C with 4.2% humidified Ar gas mixed with 200 ppm oxygen gas for 3 h and finally oxygenated at 500 °C for 1.5 h in pure oxygen gas atmosphere. Consequently, YBCO films consisting of BZO and Y_2O_3 with thickness of 200 nm were obtained.

The film thickness was measured with a Dektak step profiler. The surface morphology of YBCO film was observed by field emission scanning electron microscopy (FESEM, FEI-Siron). The phase and texture of the as-grown film was characterized by X-ray diffraction (XRD) using Cu-Kα radiation (Philips X' Pert MRD). Resistive T_c values were measured by a standard four-probe method and J_c values in self field were measured by J_c-scan Leipzig system. The critical current density in magnetic fields along the *c*-axis of YBCO was determined from DC magnetization loops of rectangular samples by measurements on a Quantum Design Magnetic Properties Measurement System (MPMS-XL) in DC field up to 9 T. The J_c values of the YBCO films in magnetic fields were determined using the Bean critical state model

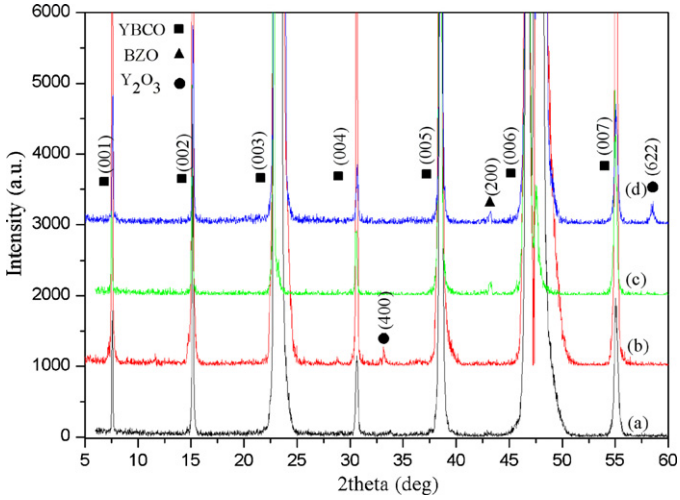

Fig. 2. XRD θ–2θ diffraction patterns of YBCO films prepared with different solutions: (a) conventional TFA precursor solution, (b) 7 mol.% excess acetates of yttrium TFA precursor solution, (c) 7 mol.% Zr acetylacetonate TFA precursor solution, and (d) 7 mol.% excess acetates of yttrium and 7 mol.% Zr acetylacetonate TFA precursor solution.

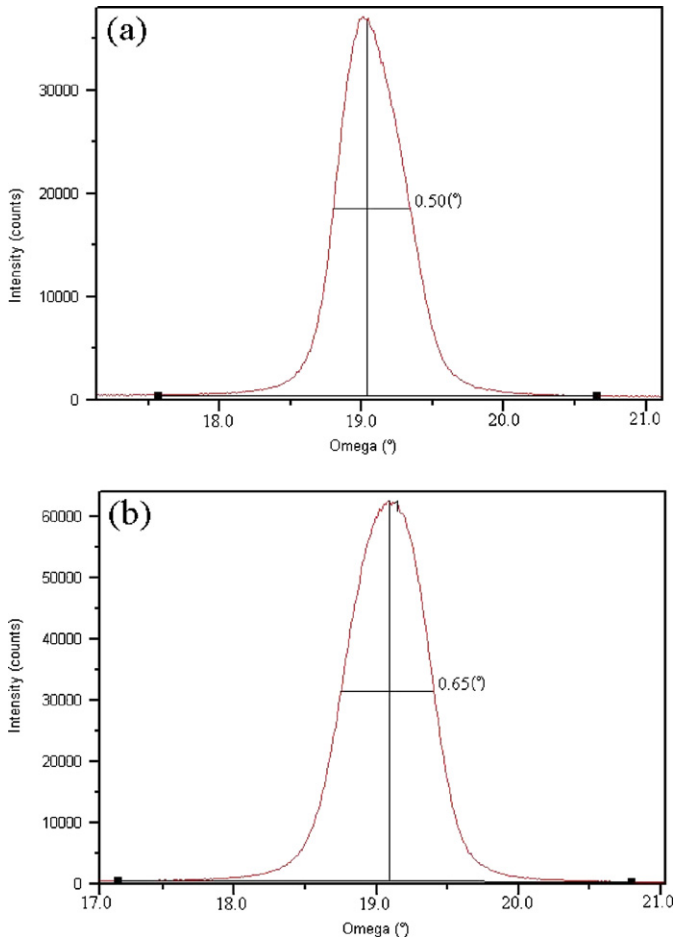

Fig. 3. (0 0 5) omega-scan of the YBCO film prepared with different solutions: (a) conventional TFA precursor solution and (b) 7 mol.% excess acetates of yttrium and 7 mol.% Zr acetylacetonate TFA precursor solution.

formula, $J_c(H) = 20\Delta M(H)/n{\cdot}a{\cdot}b{\cdot}a(1-(a/3b))$, where ΔM is the vertical width of the volume magnetization (emu cm^{-3}), n is the thickness of sample, a and b (cm) are the cross-sectional dimensions of the sample perpendicular to the applied field with $b \geq a$.

3. Results and discussion

Fig. 1 shows the SEM micrographs of the YBCO films prepared using different precursor solutions with the same heat treatment schedule. It can be seen that their surface morphologies were significantly different from each other. A smooth surface with few particles was observed in the whole area of pure YBCO film, as shown in Fig. 1a. The micrograph of YBCO film prepared using the 7.0 mol.% excess acetates of yttrium TFA precursor solutions was shown in Fig. 1b. Nanoparticles with lateral dimension of 50–100 nm can be clearly seen on the surface of the sample. The dimensions of particles in the film prepared using the 7.0 mol.% Zr acetylacetonate TFA precursor solution are observed between 20 and 50 nm, the longer of which are formed by fusing smaller units together, as shown in Fig. 1c. Fig. 1d shows the SEM micrograph of YBCO film prepared using the 7.0 mol.% excess acetates of yttrium and 7.0 mol.% Zr acetylacetonate TFA precursor solutions. The density of particles on the YBCO film surface is larger than other samples. Interestingly, the dimension of the particles becomes smaller (the size of the particles is between 10 and 40 nm, as shown in Fig. 1e). And these particles (the bright phase) are observed to be distributed uniformly across the film surface rather than clustered together.

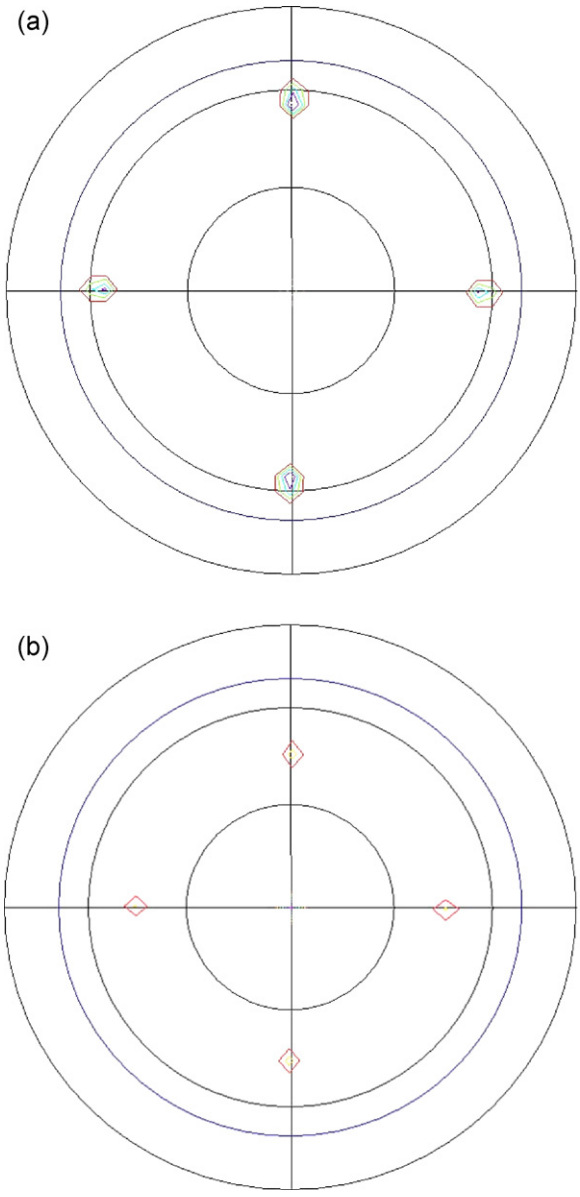

Fig. 4. Texture measurement of (a) YBCO (1 0 2) and (b) $BaZrO_3$ (1 1 0) pole figures on a BZO/Y_2O_3-doped sample. The $BaZrO_3$ precipitates mainly grow c-axis oriented in a cube-on-cube relationship towards the YBCO film.

Fig. 2 shows the XRD θ–2θ diffraction patterns for the same samples as in Fig. 1. It can be seen that all the major diffraction peaks can be indexed as (0 0 l) reflections of YBCO phase, which indicates a well-textured, c-axis oriented YBCO grain structure. In addition to the (0 0 l) YBCO peaks, some weak peaks were observed in Fig. 2b–d. The peak at 2θ angle of 33.791° in Fig. 2b is assigned to the Y_2O_3 (4 0 0) phase. It suggests that excess acetates of yttrium could react with oxygen to form Y_2O_3 during the conversion process. And Y_2O_3 particles grow in a c-axis orientation. The peak at 2θ angle of 43.238° in Fig. 2c is assigned to the BZO (2 0 0) phase. It reveals that the BZO particles also grow in a c-axis orientation in YBCO matrix. The two peaks at 2θ angles of 43.238° and 57.660° in Fig. 2d are assigned to the BZO (2 0 0) phase and Y_2O_3 (6 2 2), respectively. It demonstrates that the YBCO film prepared using the excess acetates of yttrium and Zr acetylacetonate TFA precursor solution formed BZO and Y_2O_3 phases. Comparing with Y_2O_3 phase in Fig. 2b, Y_2O_3 particles grow in a random orientation in Fig. 2d. The BZO has the same crystal orientation in both samples.

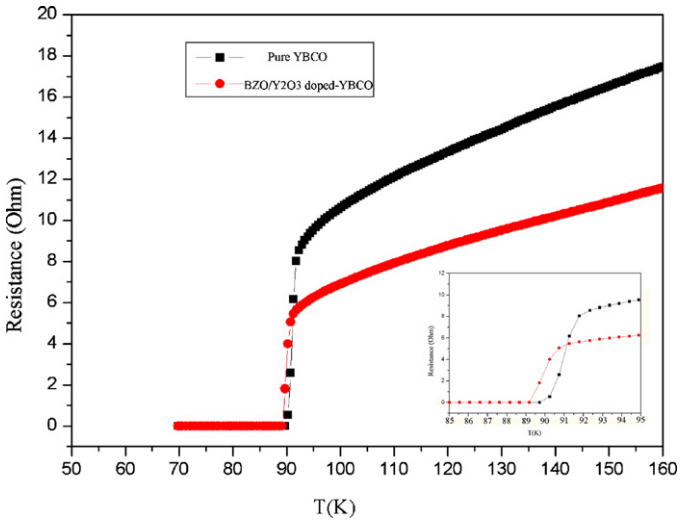

Fig. 5. Dependence of normalized resistivity R on temperature T for pure the YBCO film and the BZO/Y_2O_3-doped YBCO film.

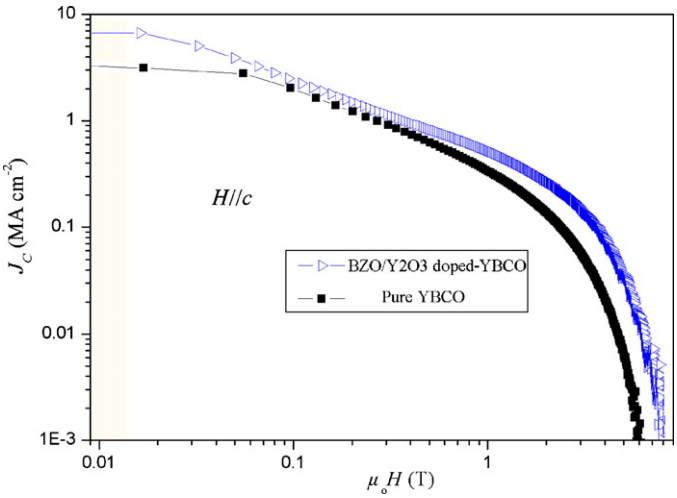

Fig. 6. Critical current density versus magnetic field parallel to the c-axis at 77 K for the pure YBCO film and the BZO/Y_2O_3-doped YBCO film.

In order to evaluate the effects of the BZO and Y_2O_3 doping on the out-of-plane orientation of the YBCO films, X-ray ω-scan was performed for the YBCO (0 0 5) reflections. The full-width-at-half-maximum (FWHM) of the (0 0 5) peaks for the pure YBCO film and YBCO films with BZO and Y_2O_3 doping are ranging typically from 0.50° to 0.65°, as shown in Fig. 3. These results indicate that the YBCO films with BZO and Y_2O_3 doping still have good out-of-plane orientation comparison with the pure YBCO films.

The in-plane orientations of the YBCO films were examined by means of (1 0 2) φ-scans. All the samples have similar results, as shown in Fig. 4a. A fourfold symmetry can be clearly seen, which confirms the presence of primarily a single in-plane orientation. Both the X-ray ω-scan and X-rayφ-scan patterns show that the YBCO films are highly c-axis-oriented, with no off-orientations. Fig. 4b shows X-ray diffraction pole figure for BZO of the typical sample prepared using the excess acetates of yttrium and Zr acetylacetonate TFA precursor solution. The four symmetric (1 1 0) BZO reflections reveal that the precipitates grow in a cube-on-cube relationship to YBCO.

T_c values of YBCO samples were measured by four probe method, as shown in Fig. 5. The T_c value of YBCO film with BZO and Y_2O_3 is about 90 K, indicating that there are little effects of BZO and Y_2O_3 particles on the YBCO matrix in these solution-derived YBCO composite films. Moreover, the transition width (ΔT) of these YBCO films was all lower than 1 K, which suggests the high homogeneity within the films.

The dependence of magnetic field on J_c values for the YBCO films with 7.0 mol.% BZO and 7.0 mol.% Y_2O_3 were investigated in comparison with that of the pure YBCO film. Fig. 6 shows the J_c values versus magnetic field (B//c-axial) at 77 K for pure YBCO film and BZO/Y_2O_3-doped YBCO films. The self-field J_c values for the un-doped YBCO film and the BZO/Y_2O_3-doped YBCO film were 3.2 mA/cm^2 and 6.5 mA/cm^2, respectively. As compared with the pure YBCO film, J_c value of the YBCO film with 7.0 mol.% BZO and 7.0 mol.% Y_2O_3 improved slightly in low field. However, J_c was improved significantly in high field (>1 T). J_c value of BZO/Y_2O_3-doped YBCO film was enhanced by a factor of 5 in 3 T field. And a significant increase in the irreversibility field H_{irr} to 8 T was observed.

Finally, we would like to put an emphasis on how the synergetic combination of BZO and Y_2O_3 to improve J_c of YBCO film. For only Y_2O_3 nanoparticles doped YBCO films, the dimension of these particles is large (50–100 nm). It is not the optimum size for effective pinning centers in YBCO films. And for only BZO nanoparticles doped YBCO films, some BZO particles clustered together. However, for BZO/Y_2O_3-doped YBCO films, the size of the particles is between 10 and 40 nm and these particles distributed uniformly across the film surface. Moreover, Y_2O_3 particles grow random oriented and BZO particles grow in a cube-on-cube relationship to YBCO. So, the strongly enhanced flux pinning over a wide range of magnetic field can be attributed to the combined different crystal structures of BZO and Y_2O_3.

4. Conclusions

It is shown that high quality BZO/Y_2O_3-doped YBCO films can be fabricated by TFA-MOD process. These BZO and Y_2O_3 structures can be combined synergistically to maximize J_c. The critical current density in magnetic fields up to 8 T reveals a strong enhancement of J_c at high magnetic fields with these different nanostructures of precipitates. And the BZO/Y_2O_3-doped YBCO films had T_c value over 90 K and ΔT lower than 1 K, indicating little effects of introduced BZO and Y_2O_3 particles on the YBCO matrix.

Acknowledgements

This work was supported by the National Natural Science Foundation of China under Contract No. 51002149 and National Basic Research Program of China (973 Program) under Contract No. 2011CBA00105.

References

[1] S.R. Foltyn, L. Civale, J.L. MacManus-Driscoll, Q.X. Jia, B. Maiorov, H. Wang, M. Maley, Nat. Mater. 6 (2007) 631.
[2] A. Crisan, S. Fujiwara, J.C. Nie, A. Sundaresan, H. Ihara, Appl. Phys. Lett. 79 (2001) 4547.
[3] T. Aytug, M. Paranthaman, A.A. Gapud, S. Kang, H.M. Christen, K.J. Leonard, P.M. Martin, J.R. Thompson, D.K. Christen, R. Meng, I. Rusakova, C.W. Chu, T.H. Johansen, J. Appl. Phys. 98 (2005) 114309.
[4] J.C. Nie, H. Yamasaki, H. Yamada, Y. Nakagawa, K. Develos-Bagarinao, Y. Mawatari, Supercond. Sci. Technol. 17 (2004) 845.
[5] A. Öztürka, İ. Düzgünb, S. Çelebi, J. Alloys Compd. 495 (2010) 104.
[6] S.V. Samoilenkov, O.V. Boytsova, V.A. Amelichev, A.R. Kaul, Supercond. Sci. Technol. 24 (2011) 055003.
[7] R.L.S. Emergo, F.J. Baca, J.Z. Wu, T.J. Haugan, P.N. Barnes, Supercond. Sci. Technol. 23 (2010) 115010.
[8] B. Maiorov, S.A. Baily, H. Zhou, O. Ugurlu, J.A. Kennison, P.C. Dowden, T.G. Holesinger, S.R. Foltyn, L. Civale, Nat. Mater. 8 (2009) 398.
[9] F. Ding, H. Gu, T. Zhang, J. Supercond. Nov. Magn. 24 (2011) 1353.
[10] T. Haugan, P.N. Barnes, R. Wheeler, F. Meisenkothen, M. Sumption, Nature 430 (2004) 867.

[11] D.M. Feldmann, T.G. Holesinger, B. Maiorov, S.R. Foltyn, J.Y. Coulter, I. Apodaca, Supercond. Sci. Technol. 23 (2010) 095004.
[12] A. Kiessling, J. Hänisch1, T. Thersleff, E. Reich, M. Weigand, R. Hühne, M. Sparing, B. Holzapfel, J.H. Durrell, L. Schultz1, Supercond. Sci. Technol. 24 (2011) 055018.
[13] P.N. Barnes, J.W. Kell, B.C. Harrison, T.J. Haugan, C.V. Varanasi, M. Rane, F. Ramos, Appl. Phys. Lett. 89 (2006) 012503.
[14] A.K. Pradhan, M. Muralidhar, Y. Feng, M. Murakami, K. Nakao, N. Koshizuka, Appl. Phys. Lett. 77 (2000) 2033.
[15] K. Develos-Bagarinao, H. Yamasaki, Supercond. Sci. Technol. 24 (2011) 065017.
[16] S.Y. Lee, S. Song, B.J. Kim, Physica C 445–448 (2006) 578.
[17] K. Nakaoka, J. Matsuda, Y. Kitoh, T. Goto, Y. Yamada, T. Izumi, Y. Shiohara, Physica C 463–465 (2007) 519.
[18] J.L. MacManus-Driscoll, S.R. Foltyn, Q.X. Jia, H. Wang, A. Serquis, L. Civale, B. Maiorov, M.E. Hawley, M.P. Maley, D.E. Peterson, Nat. Mater. 3 (2004) 439.
[19] J. Gutiérrez, A. Llordés, J. Gázquez, M. Gibert, N. Romà, S. Ricart, A. Pomar, F. Sanditmenge, N. Mestres, T. Puig, X. Obradors, Nat. Mater. 6 (2007) 367.
[20] S. Engel, T. Thersleff, R. Hühne, L. Schultz, B. Holzapfel, Appl. Phys. Lett. 90 (2007) 102505.
[21] C.V. Varanasi, P.N. Barnes, J. Burke, L. Brunke, I. Maartense, T.J. Haugan, E.A. Stinzianni, K.A. Dunn, P. Haldar, Supercond. Sci. Technol. 19 (2006) L37.
[22] C.V. Varanasi, J. Burke, L. Brunke, H. Wang, M. Sumption, P.N. Barnes, J. Appl. Phys. 102 (2007) 063909.
[23] J. Hanisch, C. Cai, R. Huhne, L. Schultz, B. Holzapfel, Appl. Phys. Lett. 86 (2005) 122508.
[24] Y. Chen, V. Selvamanickam, Y. Zhang, Y. Zuev, C. Cantoni, E. Specht, M. Parans Paranthaman, T. Aytug, A. Goyal, D. Lee, Appl. Phys. Lett. 94 (2009) 062513.
[25] P. Mikheenko, V.S. Dang1, Y.Y. Tse, M.M. AwangKechik, P. Paturi, H. Huhtinen, Y. Wang, A. Sarkar, J.S. Abell, A. Crisan, Supercond. Sci. Technol. 23 (2010) 125007.